

Unexpected Aggregation of Neutral, Xylene-Cored Dinuclear Gd^{III} Chelates in Aqueous Solution

Jérôme Costa,^[a] Edina Balogh,^[a] Véronique Turcry,^[b] Raphaël Tripier,^[b] Michel Le Baccon,^[b] Françoise Chuburu,^[b] Henri Handel,^{*[b]} Lothar Helm,^[a] Éva Tóth,^[a] and André E. Merbach^{*[a]}

Abstract: We have synthesized ditopic ligands L¹, L², and L³ that contain two DO3A³⁻ metal-chelating units with a xylene core as a noncoordinating linker (DO3A³⁻ = 1,4,7,10-tetraazacyclododecane-1,4,7-triacetate; L¹ = 1,4-bis[[4,7,10-tris(carboxymethyl)-1,4,7,10-tetraazacyclododecane-1-yl]methyl]benzene; L² = 1,3-bis[[4,7,10-tris(carboxymethyl)-1,4,7,10-tetraazacyclododecane-1-yl]methyl]benzene; L³ = 3,5-bis[[4,7,10-tris(carboxymethyl)-1,4,7,10-tetraazacyclododecane-1-yl]methyl]benzoic acid). Aqueous solutions of the dinuclear Gd^{III} complexes formed with the three ligands have been investigated in a variable-temperature, multiple-field ¹⁷O NMR and ¹H relaxivity study. The ¹⁷O longitudinal relaxation rates measured for the [Gd₂L¹⁻³(H₂O)₂] complexes show strong field dependence (2.35–9.4 T), which unambiguously proves the presence of slowly tumbling entities in solution. The proton relaxivities of the complexes, which are unexpectedly high for their molecular

weight, and in particular the relaxivity peaks observed at 40–50 MHz also constitute experimental evidences of slow rotational motion. This was explained in terms of self-aggregation related to hydrophobic interactions, π stacking between the aromatic linkers, or possible hydrogen bonding between the chelates. The longitudinal ¹⁷O relaxation rates of the [Gd₂L¹⁻³(H₂O)₂] complexes have been analysed with the Lipari-Szabo approach, leading to local rotational correlation times τ_1^{298} of 150–250 ps and global rotational correlation times τ_g^{298} of 1.6–3.4 ns (c_{Gd} : 20–50 mM), where τ_1^{298} is attributed to local motions of the Gd segments, while τ_g^{298} describes the overall motion of the aggregates. The aggregates can be partially disrupted by phosphate addition; however, at high concentrations phosphate inter-

feres in the first coordination sphere by replacing the coordinated water. In contrast to the parent [Gd(DO3A)(H₂O)_{1.9}], which presents a hydration equilibrium between mono- and dihydrated species, a hydration number of $q = 1$ was established for the [Ln₂L¹⁻³(H₂O)₂] chelates by ¹⁷O chemical shift measurements on Ln = Gd and UV/Vis spectrophotometry for Ln = Eu. The exchange rate of the coordinated water is higher for [Gd₂L¹⁻³(H₂O)₂] complexes ($k_{\text{ex}}^{298} = 7.5\text{--}12.0 \times 10^6 \text{ s}^{-1}$) than for [Gd(DOTA)(H₂O)]⁻. The proton relaxivity of the [Gd₂L¹⁻³(H₂O)₂] complexes strongly decreases with increasing pH. This is related to the deprotonation of the inner-sphere water, which has also been characterized by pH potentiometry. The protonation constants determined for this process are $\log K_{\text{OH}} = 9.50$ and 10.37 for [Gd₂L¹(H₂O)₂] and [Gd₂L³(H₂O)₂], respectively.

Keywords: cyclen • gadolinium • imaging agents • macrocycles • water exchange

[a] Dr. J. Costa, E. Balogh, Dr. L. Helm, Dr. É. Tóth, Prof. A. E. Merbach
Ecole Polytechnique Fédérale de Lausanne (EPFL)
Laboratoire de Chimie Inorganique et Bioinorganique
EPFL-BCH, 1015 Lausanne (Switzerland)
Fax: (+41)21-693-9875
E-mail: andre.merbach@epfl.ch

[b] Dr. V. Turcry, Dr. R. Tripier, Dr. M. Le Baccon, Dr. F. Chuburu, Prof. H. Handel
UMR CNRS 6521
"Chimie, Electrochimie Moléculaire et Analytique"
Université de Bretagne Occidentale, C.S. 93837

6 avenue Victor Le Gorgeu, 29238 Brest Cedex 3 (France)
Fax: (+33)298-0170-01
E-mail: henri.handel@univ-brest.fr



Supporting information for this article is available on the WWW under <http://www.chemeurj.org>; Data for FAB-MS, NMR spectra, and elemental analysis for L¹⁻³; equations used in the analysis of ¹⁷O NMR and NMRD data; variable-temperature transverse and longitudinal ¹⁷O relaxation rates and chemical shifts of [Gd₂L¹⁻³(H₂O)₂] and reference solutions; variable-temperature NMRD profiles of [Gd₂L¹⁻³(H₂O)₂]; proton relaxivities of [Gd₂L¹(H₂O)₂] at variable concentrations of Gd³⁺, PBS, and pH; UV/Vis spectra of [Eu₂L²(H₂O)₂].

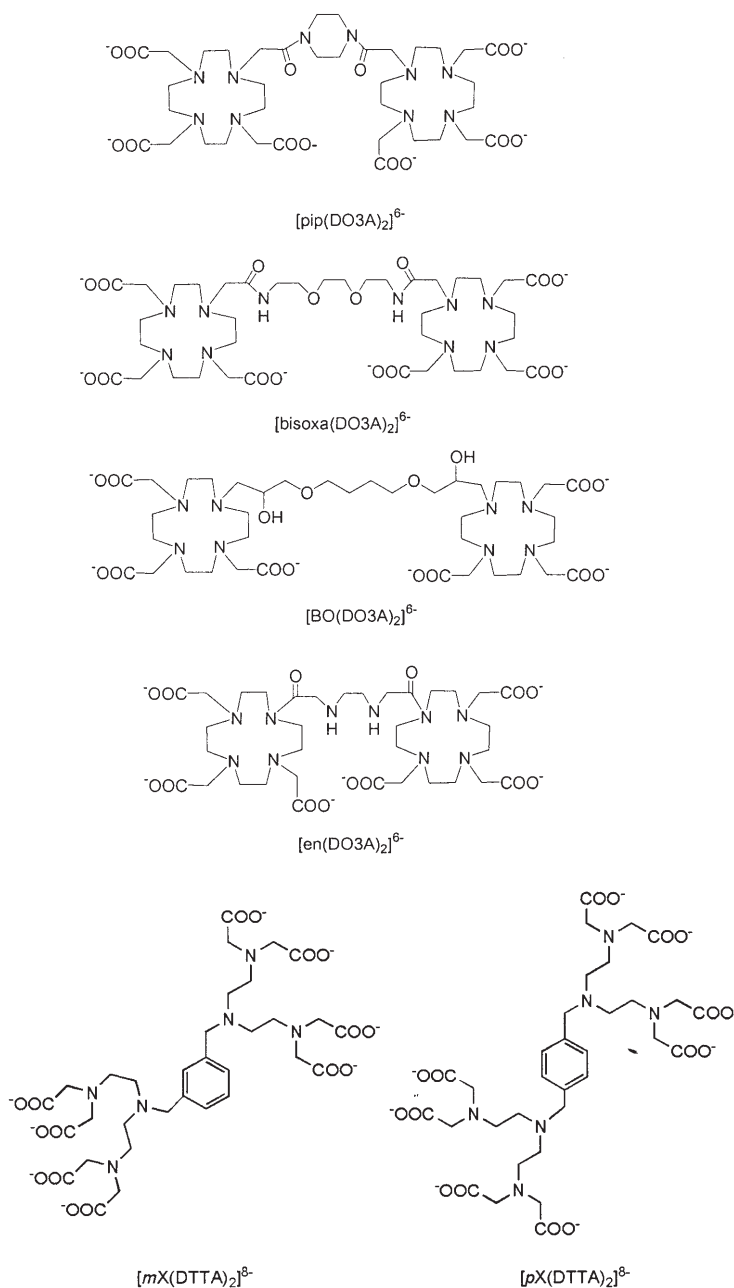
Introduction

The evolution of magnetic resonance imaging (MRI) into one of the most powerful clinical diagnostic techniques has been largely assisted by the concomitant development of contrast-enhancing agents, mainly Gd^{III} complexes.^[1] These intravenously injected paramagnetic drugs catalyze the relaxation of water protons in the tissues and hence contribute to the great resolution of the magnetic resonance images. In the last two decades, the use of Gd^{III} complexes as MRI contrast agents as well as other biomedical applications involving rare-earth ions prompted a revival of lanthanide coordination chemistry. Cyclen-based macrocyclic Ln^{III} complexes have been widely investigated: they have been found to have extremely high thermodynamic and kinetic stability,^[2,3] both very important for in vivo applications of metal complexes. $[Gd(DOTA)]^-$ is indeed a safe MRI contrast agent, while ^{90}Y complexes of DOTA-derivatives are successfully used in internal radiotherapy.^[4]

Dinuclear Gd^{III} chelates, both macrocyclic and acyclic, have been investigated in the context of contrast agent development.^[5–8] The increased molecular size of a dimer with regard to a monomer gives rise to slower rotational motion, which is favourable for contrast agent efficacy, although this improvement is often negligible in comparison to the macromolecular systems that have been proposed for MRI contrast agent purposes. Some of the formerly reported dinuclear chelates were derived from the triacetate macrocyclic DO3A³⁻ ligand in which the hydrogen atom on the fourth nitrogen has been replaced by a linker that bridges the two chelating subunits. A carbonyl ($[pip(DO3A)_2]^{6-}$, $[bisoxa(DO3A)_2]^{6-}$, $[en(DO3A)_2]^{6-}$) or hydroxyl ($[BO(DO3A)_2]^{6-}$) group has been introduced on the linker to ensure eight donor atoms (Scheme 1).

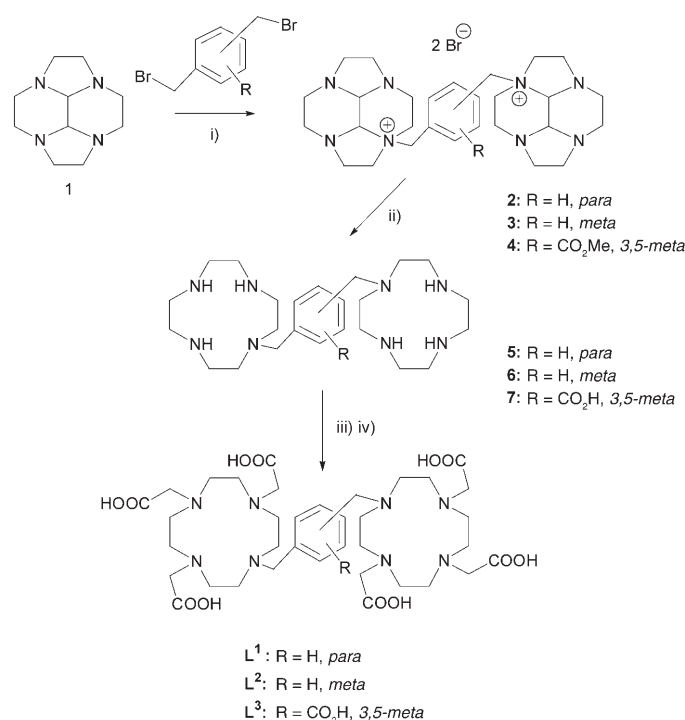
All Gd^{III} polyaminocarboxylate complexes currently used as MRI contrast agents have one inner-sphere water molecule. Its exchange rate is an important factor in determining proton relaxivity, and has been measured for numerous Gd^{III} chelates^[1] (relaxivity is defined as the paramagnetic enhancement of the water proton longitudinal relaxation rate induced by 1 mM concentration of the agent). Increasing the number of inner-sphere water molecules (q) could be beneficial for proton relaxivity, since the inner-sphere contribution is linearly proportional to q . Indeed, remarkably high proton relaxivities were recently found for dihydrated, dinuclear Gd^{III} complexes of heptadentate diethylenetriamine-tetraacetates linked to a xylene core ($[pX(DTTA)_2]^{8-}$ and $[mX(DTTA)_2]^{8-}$; Scheme 1).^[9] These high relaxivities have been attributed to the presence of two inner-sphere water molecules and to the rigidity of the dimer ligand.

Here we report the synthesis of three ditopic ligands L^1 , L^2 , and L^3 , which are derived from DO3A³⁻ and have a xylene entity as their linker (Scheme 2). No additional coordinating function has been introduced in the linker, so the heptadentate N_4O_3 chelating unit could theoretically leave space for up to two inner-sphere water molecules, based on an analogy to $[Ln(DO3A)(H_2O)_q]$ complexes.^[10]



Scheme 1. Ligands previously used for the formation of dinuclear Gd^{III} complexes.

The three dinuclear Gd^{III} complexes of L^{1-3} have been investigated in a multiple-field, variable-temperature ^{17}O NMR and 1H NMRD study with the objective of determining the main factors that influence proton relaxivity: water exchange, rotation, and electronic relaxation. The hydration number q of the Ln^{III} chelates of the three L^{1-3} ligands has been also assessed. In addition, we have identified an aggregation phenomenon in aqueous solution for these neutral Gd^{III} complexes, which strongly influences their ^{17}O and 1H relaxation behaviour. Attempts have been made to disrupt these aggregates.

Scheme 2. Synthesis of L¹⁻³.

Results and Discussion

Ligand synthesis: We recently described a simple synthesis of bis-macrocycles using bis-aminal intermediates.^[11] Lanthanide complexation necessitates the introduction of six supplementary acetate moieties, obtained for instance by direct reaction of the bis-macrocycle with an ester halide, followed by hydrolysis. Following this method, only four steps are required to obtain DO3A-based dimers starting from “cyclen-glyoxal” **1**. The *para*-xylylene-bis(*N,N'*-cyclen) **5**, *meta*-xylylene-bis(*N,N'*-cyclen) **6**, and 3,5-bis(cyclen-1-ylmethyl)-benzoic acid **7** were alkylated as ethyl esters to give the derivatives L¹⁻³ in good overall yields (L¹, 35%; L², 33%; L³, 20%; Scheme 2).

Ligands L¹ and L² consist of two DO3A moieties linked with a xylenyl center in the *para* and *meta* positions. The third dimer derived from the *meta* ligand presents a carboxylic function on the aromatic group and the two cyclen moieties in the 3,5 positions. This function results from the linker precursor: by bromination of the methyl 3,5-dimethylbenzoate, the 3,5-bis(bromomethyl)benzoic acid methyl ester was obtained and then classically used for the synthesis of the diammonium salt **4**. Hydrolysis of the methylic ester functions occurred during the deprotection step with hydrazine monohydrate to give the bis-macrocycle **7**. The following alkylation procedure remains unchanged.

¹⁷O NMR and ¹H NMRD measurements: With the objective of evaluating the parameters that determine proton relaxivity for the three dinuclear Gd^{III} complexes, we performed a variable-temperature, multiple-field ¹⁷O NMR and ¹H

NMRD (nuclear magnetic relaxation dispersion) study. ¹⁷O longitudinal and transverse relaxation rates and chemical shifts were measured in aqueous solutions of [Gd₂L¹⁻³(H₂O)_{2q}] at 4.7 and 9.4 T; for [Gd₂L¹(H₂O)_{2q}] and [Gd₂L²(H₂O)_{2q}] additional longitudinal relaxation rates were obtained at 2.35 T. Variable-temperature proton relaxation rates were measured at three temperatures (5, 25, and 37 °C).

Hydration number: For [Gd₂L¹⁻³(H₂O)_{2q}], one could expect a hydration equilibrium between *q* = 1 and 2, based on the analogy to [Ln(DO3A)(H₂O)_q] complexes, which have an average *q* of 1.88 at 298 K.^[10] There is no direct way to check the presence of a hydration equilibrium for a Gd^{III} complex. Hydration equilibria are easily characterized by the UV/Vis absorption spectrum of the neighbouring Eu^{III}, which has a ⁷F₀→⁵D₀ transition band around 578–582 nm that is very sensitive to the coordination environment.^[10,12,13] Hydration numbers can be assessed by laser-induced luminescence, based on the difference in luminescence lifetimes measured in H₂O and D₂O solutions.^[14] Furthermore, lanthanide-induced shifts (LIS) are commonly applied to determine *q*.^[15] This method often uses Dy^{III} complexes; however, it is also applicable to Gd^{III} analogues. The Gd^{III}-induced ¹⁷O chemical shifts measured in the fast exchange region are directly proportional to the number of coordinated water molecules for a given concentration of Gd. By using a commonly used value for the hyperfine coupling constant, *A/h* (−3.8 × 10⁶ rad s^{−1}), one can calculate *q*. In practice, it is usually *A/h* that is calculated from the ¹⁷O chemical shifts by assuming and fixing *q* in the fit. If the value of the scalar coupling constant obtained in this way is in the common range,^[16] the assumed *q* was correct, if not, the hydration number used in the calculations can be suspected to be wrong.

For all three dinuclear chelates, the ¹⁷O chemical shifts are compatible with *q* = 1 ± 0.2. Therefore, the ¹⁷O NMR and NMRD data for all three Gd^{III} chelates have been analysed by assuming *q* = 1. We obtain reasonable values for *A/h*, whereas inconceivably low values would be calculated with *q* = 2. We thus conclude that the three [Gd(H₂O)_q]₂L¹⁻³ complexes are monohydrated.

Recently, Faulkner and co-workers reported a luminescence study on [Ln(H₂O)_q]₂L¹ complexes,^[17] and found *q* = 1.9 for [Eu₂L¹(H₂O)_{2q}] and [Tb₂L¹(H₂O)_{2q}] and *q* = 0.4 for [Yb₂L¹(H₂O)_{2q}]. This would mean two bands in the UV/Vis absorption spectrum of [Eu₂L¹(H₂O)_{2q}], characteristic of the hydration equilibrium. However, a variable-temperature UV/Vis study performed on [Eu₂L¹⁻³(H₂O)_{2q}] complexes showed a temperature-invariant absorption band with a shoulder for [Eu₂L¹(H₂O)_{2q}] and [Eu₂L³(H₂O)_{2q}], and a relatively symmetrical band for [Eu₂L²(H₂O)_{2q}] (Figure 1). In a hydration equilibrium, the two bands belonging to the differently hydrated species display opposite temperature behaviour: as the temperature increases, the intensity of the least hydrated complex increases while the other decreases. In contrast, no temperature dependence is observed for

$[\text{Eu}_2\text{L}^{1-3}(\text{H}_2\text{O})_{2q}]$. Moreover, the absorption bands originating from different hydration modes are generally less broad and more separated (typically by ~ 0.5 – 0.8 nm) than those observed here.^[10,12,13] In the case of $[\text{Eu}_2\text{L}^1(\text{H}_2\text{O})_{2q}]$ and $[\text{Eu}_2\text{L}^3(\text{H}_2\text{O})_{2q}]$, the separation of the shoulder from the main peak is less than 0.4 nm. Based on these considerations, and more importantly on the temperature invariance of the visible spectrum, we conclude that no hydration equilibrium exists for these dinuclear complexes.

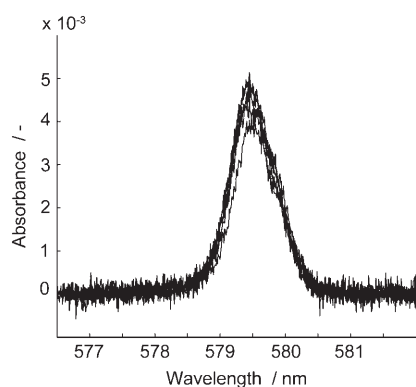


Figure 1. Superposition of UV/Vis absorption spectra of $[\text{Eu}(\text{H}_2\text{O})_q]\text{L}^1$ at six different temperatures between 16.8 and 76.3 °C (the position of the bands was normalized to the maximum of the 25.5 °C spectrum).

Recently, pH-dependent hydration numbers have been reported for a series of DO3A-derived lanthanide complexes, for which the pH-dependence was rationalized by dimerization of the chelates, induced by a bridging carboxylate group.^[18] At pH 8 (deprotonated carboxylate coordinates to Ln^{3+} of a neighbouring complex) $q = 1$, while at pH 2 (protonated and noncoordinating carboxylate) $q = 2$ was determined for the europium(III) analogue, with an overall coordination number of 9 in each case.

Parker and co-workers have recently reported on DO3A derivatives bearing N-linked $(\text{CH}_2)_n$ -NHCO-pyridyl moieties. By changing the length (n) of the substituent, they could control the hydration state of the Eu^{III} and Gd^{III} complexes, which were monohydrated for $n = 2$ and had no inner-sphere water for $n = 3$, as evidenced by luminescence and relaxometric measurements.^[19] On the basis of solid-state infrared spectra, they assumed coordination of the amide oxygen for both $n = 2$ and 3 complexes, which implies a seven- and eight-membered chelate ring, respectively. Given the very low stability of such large chelate rings, we think amide coordination is not necessarily present in the solution state. This would imply an eight-coordinate state of the lanthanide ion with one inner-sphere water molecule, similar to the structure assumed for our dinuclear systems.

Aggregation: For all three complexes, the ^{17}O longitudinal relaxation rates show strong field dependence (Figure 2), which imperatively points to slow rotational motion. The

size of the $[\text{Gd}_2\text{L}^{1-3}(\text{H}_2\text{O})_{2q}]$ complexes is not large enough to account for this behaviour, and no T_1 field-dependence has been previously found for complexes of similar size. This observation can only be explained by the formation of aggregates in aqueous solution. These dinuclear complexes are neutral (even in $[\text{Gd}_2\text{L}^3(\text{H}_2\text{O})_{2q}]$ only a negligible fraction of the central COOH is deprotonated at the pH of the measurement, see below). The aggregation phenomena could result from hydrophobic interactions, π stacking between the aromatic linker, and possible hydrogen bonding between the chelates. No aggregation has been found for the previously reported neutral dinuclear Gd^{III} complexes, such as $[\text{Gd}_2(\text{pip}(\text{DO3A})_2)]$, $[\text{Gd}_2(\text{bisoxa}(\text{DO3A})_2)]$, or $[\text{Gd}_2(\text{BO}(\text{DO3A})_2)]$, which is probably related to their non-aromatic linker. Furthermore, the proton relaxivities are also remarkably high for all three $[\text{Gd}_2\text{L}^{1-3}(\text{H}_2\text{O})_{2q}]$ complexes, and more importantly, present high-field relaxivity maxima typical of slowly rotating systems (Figure 3). Again, such distinct high-field relaxivity peaks have not previously been observed for dinuclear chelates.

One cannot exclude the influence of the aggregation process on the hydration state, either. Certain water binding sites in the interior of the aggregates might not be accessible to bulk water, whereas the exterior chelates could be dihydrated (as expected for a DO3A-chelate), and on average the effective q could equal 1. The ^{17}O chemical shifts and scalar coupling constants calculated from the shifts are unambiguous experimental evidence for $q = 1$ as an effective hydration number. However, they do not allow us to decide between the scenario of $q = 1$ for each monomer and that of an effective q that equals 1 due to nonaccessibility of certain interior sites. UV/Vis spectra of $[\text{Eu}(\text{EDTA-PA}_2)]$ chelates at 25 and 100 mM showed a remarkable difference in the ratio of two bands, which was explained by different hydration numbers related to a concentration-dependent aggregation.^[20]

For $[\text{Yb}_2\text{L}^1(\text{H}_2\text{O})_{2q}]$, $q = 0.4$ has been reported.^[17] Although one indeed expects a smaller q for the smaller Yb^{III} as compared with Eu^{III} ($q = 1.9$), such a large difference is rather intriguing. One explanation could be the very different Ln^{III} concentration used in the two luminescence experiments: $c_{\text{Eu}} = 10 \mu\text{M}$ and $c_{\text{Yb}} = 10 \text{mM}$;^[21] a larger concentration might favour aggregation, which might then influence the hydration number. A similar concentration effect has previously been observed for different polyaminocarboxylate chelates and has been attributed to an increase of intermolecular interactions and viscosity in concentrated solutions.^[22] In our UV/Vis and ^{17}O NMR measurements, the Ln^{III} concentration was much higher than that used by Faulkner et al. in the luminescence determination of q ($\sim 25 \text{mM}$ vs $10 \mu\text{M}$), which could explain the discrepancy between the q values derived. Unfortunately, it is not possible to perform concentration-dependent ^{17}O chemical shift measurements for the $[\text{Gd}_2\text{L}^{1-3}(\text{H}_2\text{O})_{2q}]$ complexes in a large concentration range, since at low concentrations the observed paramagnetic shifts become very small and not precisely measurable.

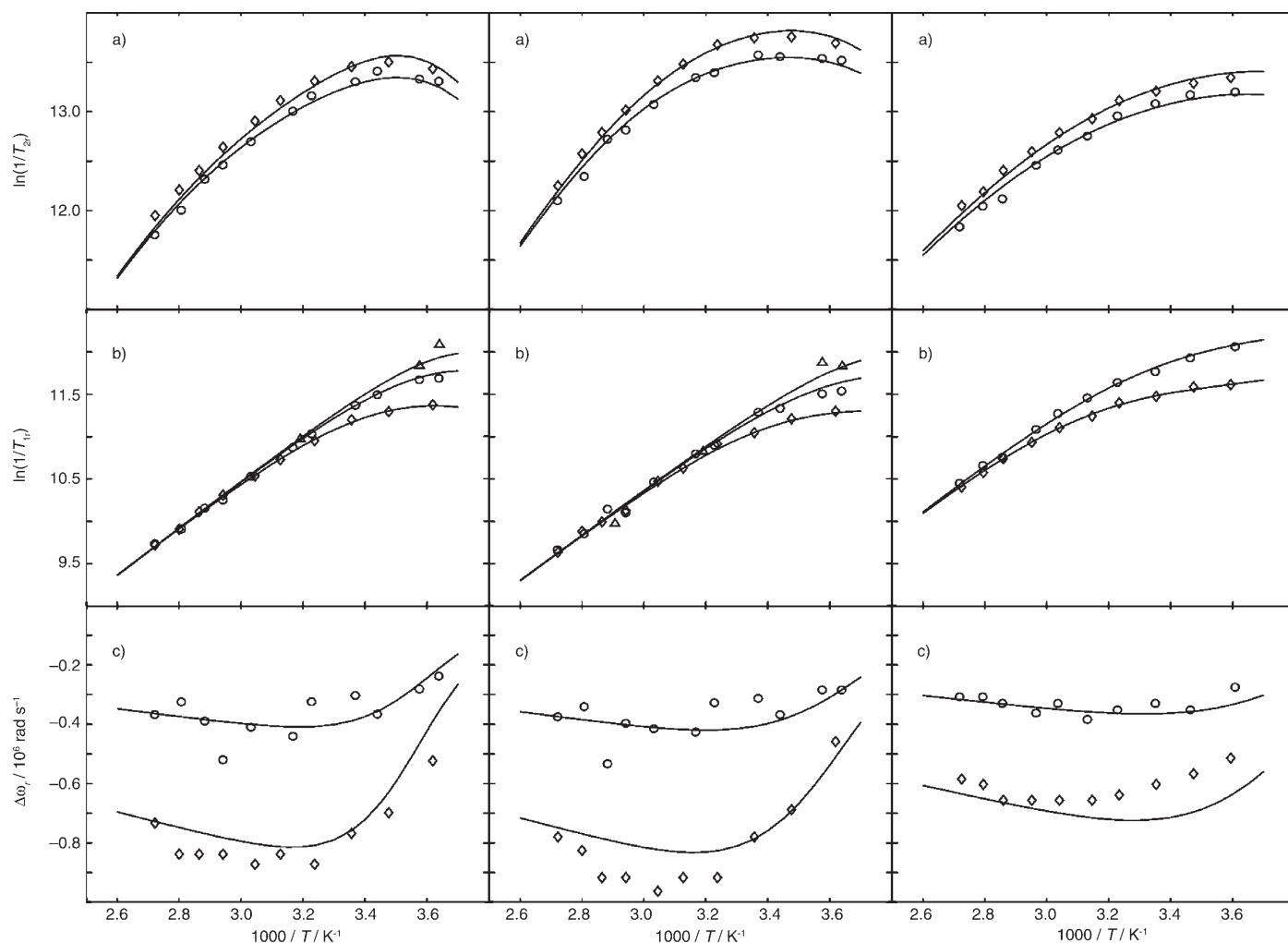


Figure 2. $[\text{Gd}_2\text{L}^1(\text{H}_2\text{O})_2]$ (left section), $[\text{Gd}_2\text{L}^2(\text{H}_2\text{O})_2]$ (middle section), and $[\text{Gd}_2\text{L}^3(\text{H}_2\text{O})_2]$ (right section): temperature dependence of reduced a) transverse $1/T_{2r}$ and b) longitudinal $1/T_{1r}$ ^{17}O relaxation rates; c) ^{17}O chemical shifts $\Delta\omega_r$, at $B = 2.35\text{ T}$ (Δ), 4.7 T (\circ), and 9.4 T (\diamond). The lines represent curves fitted to the experimental points. In the analysis, a hydration number of $q = 1$ was assumed.

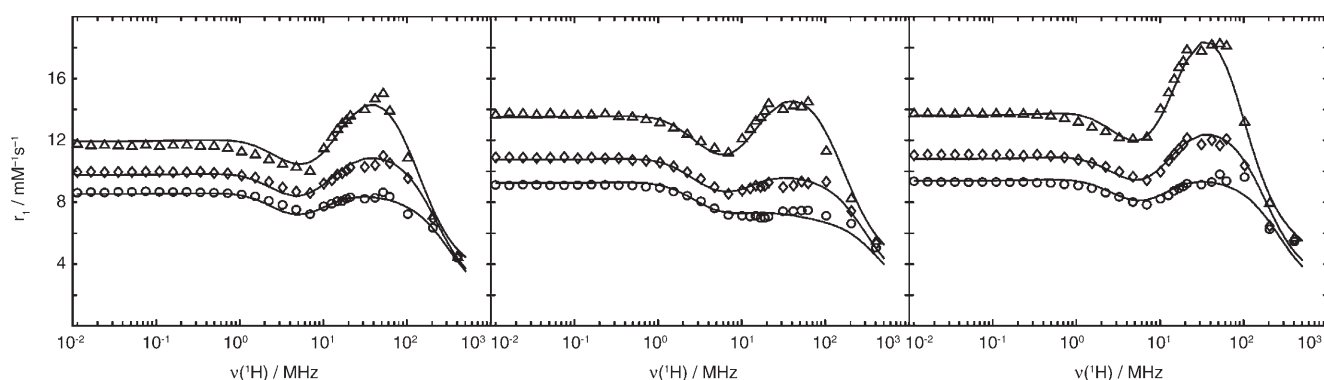


Figure 3. $[\text{Gd}_2\text{L}^1(\text{H}_2\text{O})_2]$ (left), $[\text{Gd}_2\text{L}^2(\text{H}_2\text{O})_2]$ (middle), and $[\text{Gd}_2\text{L}^3(\text{H}_2\text{O})_2]$ (right): ^1H NMRD profiles at 5°C (Δ), 25°C (\diamond), and 37°C (\circ). The lines represent curves fitted to the experimental points. In the analysis, a hydration number of $q = 1$ was assumed.

Fitting of the ^{17}O NMR and NMRD data: Given the slow rotational motion, the longitudinal ^{17}O and ^1H relaxation rates could not be analysed with a single rotational correla-

tion time. The Lipari–Szabo model-free approach^[23] has been successfully applied for the evaluation of NMR relaxation data of various MRI related macromolecular systems,

such as micellized surfactants,^[24,25] linear polymers,^[26,27] or dendrimers.^[28,29] This model assumes two kinds of motion to modulate the interaction that leads to relaxation: a rapid local motion, characterised by a correlation time τ_1 (activation energy E_1) and a slow global motion with a correlation time τ_g (activation energy E_g). The global rotational times τ_g obtained from either ^{17}O NMR or ^1H NMRD experiments represent the same overall motion of the system ($\tau_{gO} = \tau_{gH}$), while the local rotational correlation times τ_{1O} and τ_{1H} are different: they are attributed to the motion of the Gd–O_{water} and Gd–H_{water} vectors, respectively. Finally, a model-independent measure of the spatial restriction of the local motion is given by the generalized order parameter S . For an isotropic internal motion $S = 0$, while for a fully restricted motion $S = 1$.

In recent years, it has become general practice to fit ^{17}O NMR and NMRD data simultaneously, which is thought to yield more physically meaningful parameters.^[5] For any of the three dinuclear complexes, the simultaneous fit of the ^1H and ^{17}O data was not possible. This is likely the result of the aggregation phenomena, which can be fundamentally different at the different concentrations used for the two techniques. Aggregation is expected to be more important at the higher concentration of the ^{17}O NMR measurements. Indeed, the rotational correlation times obtained from ^{17}O NMR spectra are much longer than those calculated from ^1H relaxation. The water exchange rate is well defined through the ^{17}O NMR measurements, therefore the parameters describing water exchange (k_{ex}^{298} , ΔH^\ddagger , ΔS^\ddagger) were fixed in fitting the ^1H NMRD data. Only the rotational correlation times τ_g^{298} and τ_1^{298} , as well as the electronic relaxation parameters (Δ^2 , τ_v^{298}) and the spatial restriction parameter S^2 were fitted. Fitting of activation energies (E_g , E_1) was in most cases not possible owing to strong correlation; they have therefore been adjusted manually to reasonable values.

In the fitting procedure, r_{GdO} was fixed to 2.50 Å, based on available crystal structures^[30,31] and recent electron spin echo envelope modulation (ESEEM) results.^[32] The Gd^{III}–H distance r_{GdH} was set to 3.10 Å,^[5,33] the distance of closest approach of an outer-sphere water proton to the gadolinium(III) a_{GdH} to 3.5 Å,^[5] and the quadrupolar coupling constant $\chi(1+\eta^2/3)^{1/2}$ to the value for pure water, 7.58 MHz. The diffusion constant D_{GdH}^{298} used in the analysis of ^1H NMRD data was fixed to $23 \times 10^{-10} \text{ m}^2 \text{ s}^{-1}$, and its activation energy E_{GdH} to 20 kJ mol⁻¹. For the empirical constant characterizing the outer-sphere contribution to the ^{17}O chemical shifts we used $c_{\text{os}} = 0.1$.

Electronic relaxation rates $1/T_{\text{ic}}$ ($i = 1, 2$) influence both ^{17}O and ^1H relaxation of Gd^{III} complexes and are generally

governed by the zero-field splitting (ZFS) term. In the analysis, we used Powell's approach:^[5] here $1/T_{\text{ic}}$ is the sum of a transient ZFS and a spin-rotation (SR) contribution. The ZFS term is described by the trace of the squared ZFS tensor Δ^2 , a correlation time τ_v , and activation energy E_v (fixed to 1 kJ mol⁻¹). The SR term is characterized by a δg_L^2 parameter, for which the fit gave values of 0.096 ± 0.003 , 0.022 ± 0.002 , and 0.059 ± 0.002 for $[\text{Gd}_2\text{L}^1(\text{H}_2\text{O})_2]$, $[\text{Gd}_2\text{L}^2(\text{H}_2\text{O})_2]$, and $[\text{Gd}_2\text{L}^3(\text{H}_2\text{O})_2]$, respectively. It has to be noted that for τ_v the fit of NMRD gives systematically higher values as compared with the ^{17}O NMR fit. Since we know that the theory of electronic relaxation is not fully adequate, we do not interpret this difference.

The experimental ^{17}O NMR and NMRD data and the fitted curves assuming $q = 1$ are presented in Figures 2 and 3, respectively, for all three dinuclear complexes (for equations, refer to Supporting Information); the parameters calculated are reported in Table 1.

Table 1. Parameters obtained for $[\text{Gd}_2\text{L}^{1-3}(\text{H}_2\text{O})_2]$ from the independent fit of ^{17}O NMR and ^1H NMRD data. For each complex, the left and right semicolumns show the parameters calculated from ^{17}O NMR and ^1H NMRD, respectively. In the NMRD analysis, parameters of water exchange were fixed to values obtained by ^{17}O NMR. Italic values were fixed in the fit.

	$[\text{Gd}_2\text{L}^1(\text{H}_2\text{O})_2]$		$[\text{Gd}_2\text{L}^2(\text{H}_2\text{O})_2]$		$[\text{Gd}_2\text{L}^3(\text{H}_2\text{O})_2]$	
ΔH^\ddagger [kJ mol ⁻¹]	45.9 ± 1.6		41.0 ± 1.4		32.7 ± 1.5	
ΔS^\ddagger [J mol ⁻¹ K ⁻¹]	+40.7 ± 5.0		+27.5 ± 4.5		+0.3 ± 3.2	
k_{ex}^{298} [10 ⁶ s ⁻¹]	7.5 ± 0.2		11.0 ± 0.2		12.0 ± 0.3	
τ_g^{298} [ps]	1614 ± 25	889 ± 18	1677 ± 24	570 ± 11	3418 ± 30	974 ± 15
E_g [kJ mol ⁻¹]	25	25	25	24 ± 1	23 ± 1	25
τ_1^{298} [ps]	138 ± 10	34 ± 7	170 ± 11	60 ± 8	248 ± 16	83 ± 6
E_1 [kJ mol ⁻¹]	<i>15</i>	<i>15</i>	<i>15</i>	<i>15</i>	24 ± 1	<i>15</i>
S^2	0.32 ± 0.08	0.39 ± 0.07	0.24 ± 0.06	0.39 ± 0.07	0.35 ± 0.07	0.34 ± 0.07
A/\hbar [10 ⁶ rad s ⁻¹]	-3.7 ± 0.2		-3.8 ± 0.2		-3.2 ± 0.2	
τ_v^{298} [ps]	0.4 ± 0.4		0.3 ± 0.2		0.3 ± 0.3	
Δ^2 [10 ²⁰ s ⁻²]	0.14 ± 0.03	0.20 ± 0.01	0.27 ± 0.06	0.19 ± 0.01	0.40 ± 0.05	0.18 ± 0.02

Water exchange and rotational dynamics: The water exchange rates obtained are remarkably high for a neutral, monohydrated gadolinium(III) chelate; they are similar to that of $[\text{Gd}(\text{DO3A})(\text{H}_2\text{O})_{1,9}]$ ($11 \times 10^6 \text{ s}^{-1}$)^[10] and about the double of k_{ex} of the parent $[\text{Gd}(\text{DOTA})(\text{H}_2\text{O})]^-$ ($4.6 \times 10^6 \text{ s}^{-1}$).^[34] Within the family of dinuclear chelates, the gadolinium(III) complexes of L^2 and L^3 have the highest water exchange rates ever published (Table 2). The interpretation of this water exchange rate is difficult as long as we do not know if all chelates are indeed monohydrated or $q = 1$ is only an effective value. In the latter case, the k_{ex} calculated is also an effective exchange rate. The values of the activation enthalpy and entropy point to a dissociative activation mode. No variable pressure ^{17}O NMR study was performed since the pressure would certainly have an effect on the aggregation state which might, in turn, influence the electron spin relaxation in an uncontrollable manner; it then becomes impossible to evaluate the pressure dependence of the water exchange rate.

For each Gd^{III} complex, the rotational correlation times are 2–3 times shorter when obtained from the ^1H relaxation rates rather than from the ^{17}O relaxation rates. This can result from the concentration dependence of the aggrega-

Table 2. Coordination numbers (CN), hydration numbers q , water exchange rates, k_{ex}^{298} , activation enthalpies ΔH^\ddagger , activation entropies ΔS^\ddagger , activation volumes ΔV^\ddagger , and water exchange mechanism for a selection of GdL chelates.

	L	CN	q	k_{ex}^{298} [10 ⁶ ×s ⁻¹]	ΔH^\ddagger [kJ mol ⁻¹]	ΔS^\ddagger [J mol ⁻¹ K ⁻¹]	ΔV^\ddagger [cm ³ mol ⁻¹]	Mechanism	Ref.
monomers	DOTA ⁴⁻	9	1	4.6	54.5	+65	+10.5	D	34
	DO3A ³⁻	9	1.9	11.0	33.6	+2			10
	DO2A ²⁻ [a]	9	2.8	10.0	21.0	-39			10
	PDTA ⁴⁻ [b]	8	2	102	11.0	-55	-1.5	I_a	49
dinuclear complexes	[L ¹] ⁶⁻	8	1	7.5	45.9	+41			this work
	[L ²] ⁶⁻	8	1	11.0	41.0	+28			this work
	[L ³] ⁶⁻	8	1	12.0	32.7	+0			this work
	[pip(DO3A) ₂] ⁶⁻	9	1	1.5	34.2	-12		I_d	5
	[bisoxa(DO3A) ₂] ⁶⁻	9	1	1.4	38.5	+2	+2.3	I_d	5
	[BO(DO3A) ₂] ⁶⁻	9	1	1.0	30.0	-29	+0.5	I_d	6
	[pX(DTTA) ₂] ⁸⁻	9	2	9.0	45.4	+41			9
	[mX(DTTA) ₂] ⁸⁻	9	2	8.9	39.2	+24			9

[a] DO2A²⁻ = 1,4,7,10-tetraazacyclododecane-1,7-diacetate. [b] PDTA⁴⁻ = propylenediamine-N,N',N',N'-tetraacetate.

tion. Although no concentration dependence of the relaxivity was observed between 0.23–4.69 mM Gd^{III} concentration (see below), we cannot rule out a size variation of the aggregates between the ¹⁷O and ¹H NMR measurements. This hypothesis also seems to be supported by the longer global rotational correlation time τ_{gO} calculated for [Gd₂L³(H₂O)₂] (3400 ps) for which the ¹⁷O NMR measurements were performed at higher concentration ($c_{\text{Gd}} = 0.052 \text{ mol kg}^{-1}$) than the two other complexes ($\tau_{\text{gO}} = 1610$ and 1680 ps; $c_{\text{Gd}} = 0.026$ and 0.020 mol kg⁻¹ for [Gd₂L¹(H₂O)₂] and [Gd₂L²(H₂O)₂], respectively). Consequently, the rotational correlation times presented in Table 1 refer to the aggregation state at the particular concentration of the experiment. Nevertheless, they prove that these complexes unexpectedly behave as macromolecules in aqueous solution owing to aggregation phenomena.

The average number of molecules in the aggregates was roughly estimated through the Debye–Stokes equation [Eq. (1)], in which τ_{R} is the molecular rotational correlation time (τ_{g} in the Lipari–Szabo approach), k_{B} the Boltzmann constant, η the microviscosity, r_{eff} the radius of the chelate, and T the temperature:^[35]

$$\tau_{\text{R}} = \frac{4\pi\eta r_{\text{eff}}^3}{3k_{\text{B}}T} \quad (1)$$

Assuming a spherical aggregate, τ_{R} is proportional to the volume of the sphere. The τ_{g} values obtained for our aggregates (Table 1) are ~10 times larger than those of similar-size complexes,^[5,6] we thus estimate an average aggregation number of ten.

The S^2 parameter is independent of the measurement (¹H or ¹⁷O), and its low value indicates considerable internal flexibility of the aggregates.

Disaggregation: Various tests have been undertaken on [Gd₂L¹(H₂O)₂] in order to disrupt the aggregates. These tests were followed by relaxometry at 40 MHz and 298.2 K, where r_1 is governed by rotation. Proton relaxivities can be

very conveniently used as aggregation state sensors in diverse paramagnetic systems, such as gadolinium-encapsulated fullerenes^[36] or micelles (cmc determination).^[24]

On dilution of a [Gd₂L¹(H₂O)₂] solution from 4.69 to 0.23 mM, no relaxivity change was observed, indicating that the aggregation state does not change significantly in this limited concentration range. Although salts are known to disrupt aggregates in aqueous solution of diverse compounds, no relaxivity decrease was observed for [Gd₂L¹(H₂O)₂] on addition of substantial amounts of NaCl (up to 3.0 M to a 4.69 mM Gd^{III} solution). On the contrary, relaxivity increases by ~40%, most likely as a result of increasing viscosity.

In a recent study on water-soluble, malonate- or OH-derivatized gadofullerenes, we proved that phosphate-buffered saline (PBS), and phosphate in particular, are very efficient in disrupting aggregates.^[36] We related the specific effect of phosphate to the intercalation of H₂PO₄⁻ and HPO₄²⁻ ions (pH 7.4) into the hydrogen-bonding network around the malonate or OH groups of the gadofullerenes. Phosphate has a tendency to create strong hydrogen bonds. Fullerene aggregation is mainly due to hydrophobic forces, thus the intercalation of phosphate will separate the molecules and inhibit these interactions. A similar effect is operative for the dinuclear compounds: by varying the PBS concentration in [Gd₂L¹(H₂O)₂] solutions, a considerable relaxivity decrease was observed (~30% in 25 mM phosphate/375 mM NaCl). The influence of PBS was further investigated at 298.2 K over the whole range of proton Larmor frequencies (Figure 4). In 20 mM phosphate/300 mM NaCl, the low-field (<1 MHz) relaxivities, dominated by electronic relaxation, do not change, while the high-field relaxivities decrease considerably. This suggests that under these conditions the PBS does not change the hydration number of the chelate; it only reduces the extent of aggregation. It has to be noted that the decreased rotational correlation time should also diminish the low-field relaxivities, though to a smaller extent than at high field. On the other hand, disaggregation can influence the electron spin relaxation as well, and the inter-

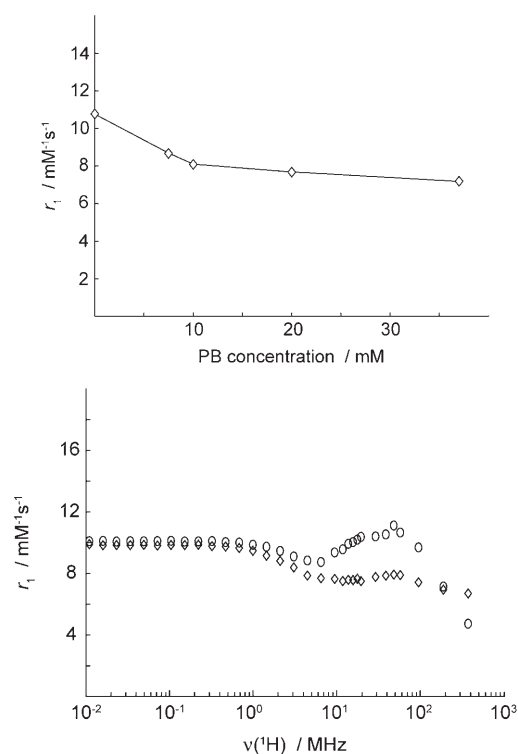


Figure 4. Top: ^1H relaxivity r_1 of $[\text{Gd}_2\text{L}^1(\text{H}_2\text{O})_2]$ as a function of PBS concentration (40 MHz, 298.2 K, $c_{\text{Gd}} = 1.36 \text{ mM}$, $c_{\text{NaCl}} = 15 \times c_{\text{phosphate}}$, pH 7.40). The line is drawn to guide the eyes. Bottom: ^1H NMRD profiles of $[\text{Gd}_2\text{L}^1(\text{H}_2\text{O})_2]$ without PBS (\circ) ($c_{\text{Gd}} = 4.30 \text{ mM}$, pH 5.82) and with PBS (\diamond) ($c_{\text{Gd}} = 2.50 \text{ mM}$, $c_{\text{phosphate}} = 20.00 \text{ mM}$, $c_{\text{NaCl}} = 300.00 \text{ mM}$, pH 7.40, 25 °C).

play of the two effects (rotation and electron spin relaxation) can result in unchanged relaxivities at low field.

Urea is one of the most widely used structure-breaking substances. In the case of $[\text{Gd}_2\text{L}^1(\text{H}_2\text{O})_2]$, it turned out to be inefficient, as indicated by the limited decrease of r_1 ($9.09 \text{ mM}^{-1}\text{s}^{-1}$ in 1 M urea, $8.79 \text{ mM}^{-1}\text{s}^{-1}$ in 3 M urea vs. $7.68 \text{ mM}^{-1}\text{s}^{-1}$ in 20 mM phosphate; 40 MHz, 25 °C).

With the objective of characterizing water exchange and rotation of the dinuclear chelates in the disaggregated state, we performed variable-temperature ^{17}O NMR measurements on a solution of $[\text{Gd}_2\text{L}^1(\text{H}_2\text{O})_2]$ containing PBS ($c_{\text{phosphate}} = 20.00 \text{ mmol kg}^{-1}$, $c_{\text{NaCl}} = 300.00 \text{ mmol kg}^{-1}$), at 4.7 and 9.4 T. An overall decrease and no more field-dependence of the $1/T_1$ values were observed, which indicates aggregate disruption and subsequent reduction of the rotational correlation time. However, the ^{17}O longitudinal relaxation rates are still higher than those measured for similar-size dinuclear chelates, indicating only partial disaggregation. On the other hand, the $1/T_2$ and $\Delta\omega$ values are only slightly affected by PBS, which suggests that water exchange and the hydration state do not change in a 20 mM PBS solution. We attempted to increase the phosphate concentration in order to reach a fully disaggregated state at a Gd^{III} concentration suitable for ^{17}O NMR (0.009 M $[\text{Gd}_2\text{L}^1(\text{H}_2\text{O})_2]$ and 0.5 M phosphate). In this sample, the measured $1/T_1$ re-

laxation rate was much shorter than in 0.020 M phosphate, as expected for more disaggregation. However, the reduced chemical shifts were only half of those without phosphate, indicating a reduced hydration number resulting from phosphate coordination. Moreover, a precipitate was observed in the solution a few hours after preparation. Phosphate coordination has been described previously for Gd-poly(amino carboxylate) complexes, stability constants of $\log K = 2.16$ and 4.8 were reported for the ternary complex formed between PO_4^{3-} and $[\text{Gd}(\text{dota})(\text{H}_2\text{O})]^-$ and $[\text{Gd}(\text{DO3A})(\text{H}_2\text{O})_{1,9}]$, respectively.^[37,38]

The interaction of phosphate and $[\text{Gd}_2\text{L}^1(\text{H}_2\text{O})_2]$ was further evidenced by ^{31}P relaxation time measurements in a sample containing 0.5 mM $[\text{Gd}_2\text{L}^1(\text{H}_2\text{O})_2]$ and 20 mM phosphate (pH 7.4; 25 °C). Both T_1 and T_2 are remarkably decreased ($T_1 = 4.59 \text{ ms}$, $T_2 = 4.02 \text{ ms}$) relative to a sample without $[\text{Gd}_2\text{L}^1(\text{H}_2\text{O})_2]$ ($T_1 = T_2 = 0.75 \text{ s}$). Under the same conditions, GdDOTA $^-$ has no effect on the ^{31}P relaxation rate ($T_2 = 0.75 \text{ s}$). These results show that phosphate interacts with $[\text{Gd}_2\text{L}^1(\text{H}_2\text{O})_2]$. Although we do not know about the nature of this interaction, the NMRD data (Figure 4) suggest that phosphate does not enter the inner coordination sphere at this concentration ratio, while ^{17}O chemical shifts indicate that it does enter at higher GdL and phosphate concentrations.

Our ultimate goal was to be able to prepare a fully disaggregated sample and characterize this in terms of hydration state, water exchange, and rotation. Phosphate is an efficient disaggregating agent; however, ^{17}O NMR requires high Gd^{III} concentrations, which require a correspondingly large amount of phosphate for disaggregation. Under such conditions, phosphate coordinates in the first sphere of the metal. The $[\text{Gd}_2\text{L}^3(\text{H}_2\text{O})_2]$ chelate has a noncoordinating carboxylate that can deprotonate and the negatively charged complex should have a lower (or no) tendency to aggregate. We therefore performed a variable pH relaxometric study on $[\text{Gd}_2\text{L}^3(\text{H}_2\text{O})_2]$, and also on $[\text{Gd}_2\text{L}^1(\text{H}_2\text{O})_2]$ for comparison. To our great surprise, the two complexes behaved identically: the relaxivities strongly decrease for both complexes between pH 6.0 and 11.0 to reach a value of $\sim 3 \text{ mM}^{-1}\text{s}^{-1}$ (40 MHz, 25 °C; samples were degassed to avoid any carbonate coordination and gave identical results as nondegassed samples) (Figure 5). Moreover, ^{17}O chemical shift and relaxation rate measurements in a $[\text{Gd}_2\text{L}^3(\text{H}_2\text{O})_2]$ solution at pH 12.5 evidenced that there is no exchanging inner-sphere water in the complex under these strongly basic conditions. The coordinated water is likely deprotonated, and the exchange of the hydroxide is much slower than that of water. The low relaxivities at high pH thus originate from a pure outer-sphere effect.

pH potentiometry: The pH-dependent process that causes the decrease in relaxivity was assessed by pH potentiometry, by titrating a solution of $[\text{Gd}_2\text{L}^1(\text{H}_2\text{O})_2]$ and $[\text{Gd}_2\text{L}^3(\text{H}_2\text{O})_2]$ with KOH (Figure 6). The titration curve of $[\text{Gd}_2\text{L}^1(\text{H}_2\text{O})_2]$ shows a base-consuming process that we attribute to the deprotonation of the coordinated water. The analysis of the

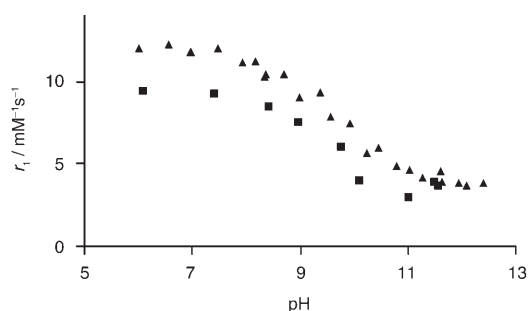


Figure 5. ¹H relaxivity r_1 of $[\text{Gd}_2\text{L}^1(\text{H}_2\text{O})_2]$ (■) and $[\text{Gd}_2\text{L}^3(\text{H}_2\text{O})_2]$ (▲) as a function of pH (at 40 MHz, 25 °C).

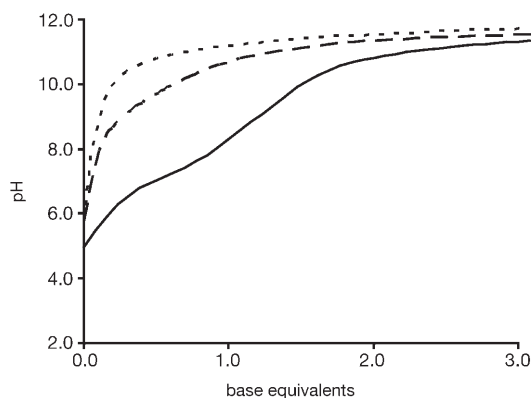


Figure 6. pH-potentiometric titration curves of $[\text{Gd}(\text{DO3A})(\text{H}_2\text{O})_{1.9}]$ (.....), $[\text{Gd}_2\text{L}^1(\text{H}_2\text{O})_2]$ (-----), and $[\text{Gd}_2\text{L}^3(\text{H}_2\text{O})_2]$ (—).

curve yielded a protonation constant of $\log K_{\text{OH}} = 9.50 \pm 0.04$.

For $[\text{Gd}_2\text{L}^3(\text{H}_2\text{O})_2]$, the titration curve is different. From pH ~6, one can also observe the deprotonation of the central carboxylate, for which we can calculate a protonation constant of $\log K_{\text{Gd}}^{\text{COOH}} = 7.1 \pm 0.06$. As expected, in lanthanide (and likely any metal) complexes this central carboxylate is not coordinated to the metal ion. The pH-potentiometric titration of the Ln_2L^3 complex is indeed a simple means of proving the noncoordination of the carboxylate. In addition to the deprotonation of the central carboxylate, we also observe another deprotonation step on the titration curve. This process, analogously to $[\text{Gd}_2\text{L}^1(\text{H}_2\text{O})_2]$, is attributed to the deprotonation of the coordinated water, with $\log K_{\text{OH}} = 10.37 \pm 0.03$, a constant somewhat higher than that for $[\text{Gd}_2\text{L}^1(\text{H}_2\text{O})_2]$. For the sake of comparison, we have also titrated a $[\text{Gd}(\text{DO3A})(\text{H}_2\text{O})_{1.9}]$ solution which showed no deprotonation in the pH 7–11 range (Figure 6). Accordingly, no relaxivity change was observed for $[\text{Gd}(\text{DO3A})(\text{H}_2\text{O})_{1.9}]$ in the pH 4–10.5 range.^[39]

We also performed pH-potentiometric titrations of the free ligand L^3 . The protonation constants of the ligand $\log K_{\text{H}_i}$ were calculated by considering the system as the sum of two identical DO3A^{3-} units (for which two amine and two carboxylate protonation constants $\log K_{\text{H}_{1-4}}$ were calculated) and one COO^- -containing ligand (protonation constant $\log K_{\text{COOH}}$). The protonation constants obtained are

presented and compared with those of analogue ligands in Table 3. The first two constants calculated for the DO3A^{3-} macrocycle, $\log K_{\text{H}_1}$ and $\log K_{\text{H}_2}$, can be attributed to the pro-

Table 3. Protonation constants in 0.1 M KCl. Values in parenthesis represent one standard deviation.

	$\text{L}^{3[\text{a}]}$	DOTA ^[b]	DO3A ^[c]
$\log K_{\text{H}_1}$	11.06 (0.04)	11.14	11.59
$\log K_{\text{H}_2}$	9.30 (0.04)	9.69	9.24
$\log K_{\text{H}_3}$	4.52 (0.06)	4.85	4.43
$\log K_{\text{H}_4}$	3.03 (0.05)	3.95	3.48
$\log K_{\text{COOH}}$	6.45 (0.11)	–	–

[a] The $\log K_{\text{H}_{1-4}}$ protonation constants were calculated by assuming two identical DO3A^{3-} units in L^3 . [b] Ref. [50]. [c] 0.1 M $(\text{CH}_3)_4\text{NNO}_3$; ref. [51].

tonation of two opposite macrocycle nitrogens, as for all cyclen-based macrocyclic ligands, then the two protonation steps characterized by $\log K_{\text{H}_3}$ and $\log K_{\text{H}_4}$ occur on two carboxylates attached to the macrocycle. The values determined for L^3 are in good accordance with those previously reported for DOTA^{4-} and DO3A^{3-} . The central carboxylate has a relatively high protonation constant, well distinct from $\log K_{\text{H}_3}$ and $\log K_{\text{H}_4}$ but somewhat lower than in the Gd^{III} complex.

Conclusion

The field-dependence of the ¹⁷O longitudinal relaxation rates unambiguously indicated the presence of slowly tumbling entities in aqueous solution of dinuclear $[\text{Gd}_2\text{L}^{1-3}(\text{H}_2\text{O})_2]$ complexes, which we attributed to self-aggregation. As driving force of the aggregation phenomenon, hydrophobic interactions, π -stacking between the aromatic linkers, and possible hydrogen bonding between the chelates can be evoked. The aggregation results in high-field proton relaxivity peaks for these complexes, typical of slow rotational motion. At frequencies where rotation dominates the relaxivity, remarkable proton relaxivities are measured, twice as high as for nonaggregated complexes of similar size. The aggregates can be partially disrupted by addition of phosphate; however, at high concentrations, phosphate interferes in the first coordination sphere by replacing the coordinated water.

In contrast to the parent $[\text{Gd}(\text{DO3A})(\text{H}_2\text{O})_{1.9}]$, which presents a hydration equilibrium between mono- and dihydrated species, a hydration number of $q = 1$ was established for all three $[\text{Gd}_2\text{L}^{1-3}(\text{H}_2\text{O})_2]$ chelates by ¹⁷O chemical shift measurements.

The proton relaxivity of the $[\text{Gd}_2\text{L}^1(\text{H}_2\text{O})_2]$ complexes strongly decreases with increasing pH. This is related to the deprotonation of the inner-sphere water, which has also been characterized by pH-potentiometry.

Experimental Section

General: All reagents were of commercial quality and solvents were dried using standard procedures. Elemental analyses were performed at the Service de Microanalyse, CNRS, 91198 Gif sur Yvette, France. Mass spectrometry analyses were performed at the Centre Régional de Mesures Physiques de l'Ouest, Rennes, France. Syntheses of all three starting bis-macrocylic ligands were performed according to the previous bis-aminal procedure^[1] using α,α' -dibromo-*para*-xylyl (for **2**, **5**, L¹ syntheses), α,α' -dibromo-*meta*-xylyl (for **3**, **6**, L² syntheses), and 3,5-bis-bromomethyl-benzoic acid methyl ester (for **4**, **7**, L³ syntheses). The synthesis of this last bis-electrophile was inspired from literature methodologies.^[40]

3,5-Bis(bromomethyl)benzoic acid methyl ester: Methyl 3,5-dimethylbenzoate (2 g, 12.2 mmol), *N*-bromosuccinimide (4.76 g, 26.8 mmol, 2.2 equiv), and a catalytic quantity of benzoyl peroxide were dissolved in carbon tetrachloride (45 mL). The mixture was stirred and heated under reflux for 6 h. After cooling to room temperature and filtration, the residue was washed three times with distilled water. The organic extracts were dried over MgSO₄, filtered, and evaporated to dryness. The residue was dissolved in a minimum of dichloromethane and the compound was precipitated with hexane and recrystallised from the same solvent. Crystals were filtered, washed with hexane, and dried under vacuum. The expected linker was finally obtained as white crystals (2.11 g, 54%). ¹³C NMR (CDCl₃, 300 MHz, RT): δ = 31.9, 52.4, 130.1, 131.4, 133.9, 139.0, 65.9 ppm.

Bis-macrocycle di-ammonium salt 4: Yield: 3.78 g, 81%; ¹³C NMR (D₂O, 300 MHz, RT): δ = 46.6, 50.4, 51.0, 51.2, 54.2, 56.2, 59.9, 60.0, 63.0, 64.3 (NCH₂), 74.4, 86.2 (C_{aminal}), 132.2, 135.4, 138.4, 143.3 (Ar), 169.8 ppm (CO).

3,5-Bis(cyclen-1-ylmethyl)-benzoic acid 7: Yield: 1.83 g, 70%; ¹³C NMR (CDCl₃, 300 MHz, RT): δ = 44.9, 46.1, 46.9, 50.9, 58.4 (NCH₂), 126.1, 132.0, 133.0, 139.6 (Ar), 168.2 ppm (CO); elemental analysis calcd (%) for C₂₅H₄₆N₈O₂·8HBr·H₂O: C 25.98, H 4.88, N 9.69; found: C 25.68, H 5.09, N 9.68.

Synthesis of L¹⁻³: *para*- or *meta*-Xylylene-bis(*N,N'*-cyclen) or 3,5-bis(*N,N'*-cyclen)methyl benzoate (1.8 mmol) and anhydrous K₂CO₃ (108 mmol) were heated under reflux in dry CH₃CN (30 mL) under N₂ atmosphere. A solution of ethyl bromoacetate (10.8 mmol) in CH₃CN (30 mL) was added dropwise and the mixture was stirred under reflux for 12 h. The inorganic solid was filtered off and CH₃CN was removed under vacuum. Aqueous HCl (2 M, 10 mL) was added and the mixture was extracted with CH₂Cl₂ (3 × 15 mL). The aqueous phase was brought to pH 12 with NaOH pellets and the hexaester was extracted with CH₂Cl₂ (3 × 15 mL). The organic extracts were dried over MgSO₄, filtered, and evaporated to dryness. Hydrolysis was carried out in refluxing HCl (6 M, 15 mL) for 6 h. HCl was subsequently evaporated to give a brown oil, which was dissolved in water (5 mL), and loaded onto a cation exchange resin (Dowex 50WX8, H⁺ form). After washing with water, the residue was eluted with 0.5 M NH₃. This fraction was evaporated to dryness, dissolved in water, and loaded onto an anion exchange resin (Dowex 1X2-200, OH⁻ form). After washing with water, the product was eluted with 1 M HCOOH. The solvent was evaporated and traces of formic acid were removed by co-evaporation with water to obtain a white solid (yields with L¹, L², and L³: 40, 39, and 35%, respectively).

Data for L¹: FAB-MS (MeOH): *m/z*: 795.4253 [M+H]⁺; ¹³C NMR (D₂O, 300 MHz, 353 K): δ = 52.3, 53.0, 53.4, 57.2, 58.6, 60.5, 63.3 (NCH₂), 134.5, 137.4 (Ar), 174.4, 175.4 ppm (CO); elemental analysis calcd (%) for C₃₆H₅₈N₈O₁₂·HCl·3H₂O: C 48.84, H 7.40, N 12.66, Cl 4.00; found: C 48.95, H 7.32, N 12.75, Cl 4.58.

Data for L²: FAB-MS (MeOH): *m/z*: 795.4253 [M+H]⁺; ¹³C NMR (D₂O, 300 MHz, 353 K): δ = 51.2, 52.1, 52.5, 52.7, 52.8, 53.5, 54.1, 57.2, 58.5, 60.8, 75.8 (NCH₂), 136.6, 135.2, 135.2, 133.9 (Ar), 173.9, 175.2 ppm (CO); elemental analysis calcd (%) for C₃₆H₅₈N₈O₁₂·2HCl·4H₂O: C 46.00, H 7.29, N 11.92, Cl 7.54; found: C 46.02, H 7.31, N 11.73, Cl 10.33.

Data for L³: FAB-MS (MeOH): *m/z*: 839.4276 [M+H]⁺; ¹³C NMR (D₂O, 300 MHz, 353 K): δ = 51.9, 52.3, 53.2, 56.1, 57.1, 59.5 (NCH₂), 134.6, 135.6, 136.1 (Ar), 171.0, 173.2, 174.1 ppm (CO); elemental analysis calcd

(%) for C₃₇H₅₈N₈O₁₄·4HCl·2H₂O: C 43.54, H 6.52, N 10.98, Cl 13.89; found: C 43.69, H 6.26, N 11.00, Cl 13.25.

Sample preparation: Aqueous solutions of [Ln₂L¹⁻³(H₂O)₂] (Ln = Gd, Eu) were prepared by mixing [Ln(ClO₄)₃] and ligand solutions in stoichiometric amounts. A slight ligand excess was used, and the pH was adjusted to about 6 by adding NaOH solution. The solutions were heated for 1 h and the pH readjusted if necessary. The absence of free metal was checked with the xylenol orange test.^[41] Gadolinium-containing samples used for ¹⁷O NMR had 2% H₂¹⁷O enrichment (IsoTrade GmbH, Mönchengladbach, Germany). All concentrations were controlled after the measurements by ICP-AES.

UV/Vis spectrophotometry: The absorbance spectra were recorded on a Perkin-Elmer Lambda 19 spectrometer in thermostated cells between 16.8 and 76.3 °C for [Eu₂L¹⁻³(H₂O)₂] (*c*_{Eu} ≈ 25 mM, pH 5.8). The measurements were done with a 10 cm optical pathlength at λ = 576.5–582.0 nm.

¹⁷O NMR spectroscopy: ¹⁷O longitudinal and transverse relaxation rates and chemical shifts of [Gd₂L¹(H₂O)₂] (*c*_{Gd} = 26.53 mmol kg⁻¹, pH 5.66), [Gd₂L²(H₂O)₂] (*c*_{Gd} = 20.17 mmol kg⁻¹, pH 5.70), and [Gd₂L³(H₂O)₂] (*c*_{Gd} = 52.17 mmol kg⁻¹, pH 6.02) were measured at variable temperatures on Bruker DPX-400 (9.4 T, 54.2 MHz) and Bruker Avance-200 (4.7 T, 27.1 MHz) spectrometers. Additionally, ¹⁷O longitudinal relaxation rates were measured for [Gd₂L¹(H₂O)₂] and [Gd₂L²(H₂O)₂] on a Bruker Avance-200 console connected to a 2.35 T (13.6 MHz) cryomagnet. Acidified water (HClO₄, pH 3.7) was used as external reference. The influence of phosphate was studied by ¹⁷O NMR at variable temperatures by measuring *T*₁, *T*₂, and $\Delta\omega$ at 9.4 and 4.7 T in aqueous [Gd₂L¹(H₂O)₂] solutions (*c*_{Gd} = 10.92 mmol kg⁻¹, *c*_{phosphate} = 20 mM, *c*_{NaCl} = 0.30 M, pH 6.80; and *c*_{Gd} = 18.45 mmol kg⁻¹, *c*_{phosphate} = 0.5 M, pH 6.80). Here we used acidified saline (HClO₄ + 300 mM NaCl, pH 3.9; for reference) or 0.5 M phosphate (pH 6.8) as external references. In all measurements, the temperature was maintained by Bruker B-VT 3000 temperature control units, and was measured by a substitution technique.^[42] The samples were sealed in glass spheres adapted to 10 mm NMR tubes to avoid susceptibility corrections of the chemical shift.^[43] The longitudinal and transverse relaxation times *T*₁ and *T*₂ were obtained with the inversion-recovery^[44] and the Carr–Purcell–Meiboom–Gill^[45] spin-echo techniques, respectively.

¹H NMRD: Water proton relaxation rates of aqueous solutions containing [Gd₂L¹(H₂O)₂] (*c*_{Gd} = 4.30 mM, pH 5.82), [Gd₂L²(H₂O)₂] (*c*_{Gd} = 2.80 mM, pH 5.75), and [Gd₂L³(H₂O)₂] (*c*_{Gd} = 2.00 mM, pH 5.86) were measured at 278.2, 298.2, and 310.2 K on a Stelar Spinmaster FFC relaxometer (Fast Field Cycling: 2 × 10⁻⁴–0.47 T, corresponding to proton Larmor frequencies of 0.01–20 MHz) equipped with a VTC90 temperature control unit, on a Bruker Minispec console connected to 0.71 T (30 MHz), 0.94 T (40 MHz), and 1.41 T (60 MHz) permanent magnets, on a Bruker Avance-200 console connected to 1.18 T (50 MHz), 2.35 T (100 MHz), and 4.7 T (200 MHz) cryomagnets, and on a Bruker DPX-400 spectrometer (9.4 T, 400 MHz). PBS concentration dependence of *r*₁ between *c*_{phosphate} = 0.0–37.0 mM (constant *c*_{NaCl}/*c*_{phosphate} = 15) on [Gd₂L¹(H₂O)₂] (*c*_{Gd} = 1.36 mM, pH 7.40) was studied at 298.2 K and 0.94 T (40 MHz). The water ¹H relaxation rates were additionally measured at 298.2 K, at all frequencies, on [Gd₂L¹(H₂O)₂] PBS-aqueous solutions (*c*_{Gd} = 2.50 mM, *c*_{phosphate} = 20.00 mM, *c*_{NaCl} = 300.00 mM, pH 7.40). Concentration dependence of the relaxivity was studied on [Gd₂L¹(H₂O)₂] at 298.2 K and 0.94 T (40 MHz) by varying *c*_{Gd} between 0.23 and 4.69 mM (pH 5.88). NaCl dependence of *r*₁ was undertaken at 298.2 K and 0.94 T (40 MHz) on [Gd₂L¹(H₂O)₂] by varying *c*_{NaCl} from 0.0 to 3.0 M (*c*_{Gd} = 4.69 mM, pH 5.88). pH-dependence of the relaxivities was followed for [Gd₂L^{1,3}(H₂O)₂] (*c*_{Gd} = 1 mM) at 40 MHz, 25 °C between pH 6–12.8. All samples were placed in cylindrical sample holders. The diamagnetic corrections to the ¹H longitudinal relaxation rates were 0.55 s⁻¹ (278.2 K), 0.37 s⁻¹ (298.2 K), and 0.33 s⁻¹ (310.2 K).

pH potentiometry: The protonation constants of L³ and those of [Gd₂L¹(H₂O)₂] and [Gd₂L³(H₂O)₂] were determined by pH-potentiometric titration at 25 °C in 0.1 M KCl at 2–3 mM concentration. A Metrohm Dosimat 665 automatic burette, a combined glass electrode (C14/02-SC, reference electrode Ag/AgCl in 3 M KCl, Moeller Scientific Glass Instruments, Switzerland) and a Metrohm 692 pH/ion-meter were used for the titra-

tions. The samples (3 mL) were stirred and N₂ was bubbled through the solutions. The H⁺ concentration was obtained from the measured pH values by the correction method proposed by Irving et al.^[46] The PSE-QUAD program was used to calculate the protonation constants.^[47]

Data analysis: The least-squares fits of the ¹⁷O NMR and ¹H NMRD data and the fit of the UV/Vis absorbance spectra were performed by the Visualiseur/Optimiseur programs on a Matlab platform, version 6.5.^[48]

Acknowledgements

This work was financially supported by the Swiss National Science Foundation, the COST Office (Switzerland), the Centre National pour la Recherche Scientifique, and the Ministère de l'Éducation Nationale (France). The research was carried out in the frame of the EC COST Action D18 and the European-funded EMIL programme (LSHC-2004-503569).

- [1] *The Chemistry of Contrast Agents in Medical Magnetic Resonance Imaging* (Eds.: É. Tóth, A. E. Merbach), Wiley, Chichester, **2001**.
- [2] É. Tóth, E. Brücher, I. Lazar, I. Tóth, *Inorg. Chem.* **1994**, *33*, 4070.
- [3] E. Brücher, *Top. Curr. Chem.* **2002**, *221*, 104.
- [4] A. Heppeler, S. Froidevaux, H. R. Mäcke, E. Jermann, M. Béhé, P. Powell, M. Hennig, *Chem. Eur. J.* **1999**, *5*, 1974.
- [5] D. H. Powell, O. M. N. Dhubhghaill, D. Pubanz, L. Helm, Y. S. Lebedev, W. Schlaepfer, A. E. Merbach, *J. Am. Chem. Soc.* **1996**, *118*, 9333.
- [6] É. Tóth, S. Vauthey, D. Pubanz, A. E. Merbach, *Inorg. Chem.* **1996**, *35*, 3375.
- [7] T.-M. Lee, T.-H. Cheng, M.-H. Ou, C. A. Chang, G.-C. Liu, Y.-M. Wang, *Magn. Reson. Chem.* **2004**, *42*, 329.
- [8] E. Zitha-Bovens, L. Vander Elst, R. N. Muller, H. van Bekkum, J. A. Peters, *Eur. J. Inorg. Chem.* **2001**, 3101.
- [9] J. Costa, É. Tóth, L. Helm, A. E. Merbach, *Inorg. Chem.* **2005**, *44*, 4747.
- [10] É. Tóth, O. M. N. Dhubhghaill, G. Besson, L. Helm, A. E. Merbach, *Magn. Reson. Chem.* **1999**, *37*, 701.
- [11] M. Le Bacon, F. Chuburu, L. Toupet, H. Handel, M. Soibinet, I. Déchamps-Olivier, J.-P. Barbier, M. Aplincourt, *New J. Chem.* **2001**, *25*, 1168.
- [12] G. Geier, C. K. Jørgensen, *Chem. Phys. Lett.* **1971**, *9*, 263.
- [13] N. Graepi, D. H. Powell, G. Laurency, L. Zékány, A. E. Merbach, *Inorg. Chim. Acta* **1995**, *235*, 311.
- [14] a) W. D. J. Horrocks, D. R. Sudnick, *J. Am. Chem. Soc.* **1979**, *101*, 334; b) D. Parker, J. A. G. Williams, *J. Chem. Soc. Dalton Trans.* **1996**, 3613; c) A. Beeby, I. M. Clarkson, R. S. Dickins, S. Faulkner, D. Parker, L. Royle, A. S. de Sousa, J. A. G. Williams, M. Woods, *J. Chem. Soc. Perkin Trans. 2* **1999**, 493; d) R. M. Supkowski, W. D. J. Horrocks, *Inorg. Chim. Acta* **2002**, *340*, 44.
- [15] M. C. Alpoim, A. M. Urbano, C. F. G. C. Geraldes, J. A. Peters, *J. Chem. Soc. Dalton Trans.* **1992**, 463.
- [16] É. Tóth, L. Helm, A. E. Merbach, *Relaxivity of Gadolinium(III) Complexes: Theory and Mechanism in The Chemistry of Contrast Agents in Medical Magnetic Resonance Imaging* (Eds.: É. Tóth, A. E. Merbach), Wiley, Chichester, **2001**.
- [17] S. J. A. Pope, A. M. Kenwright, V. A. Boote, S. Faulkner, *Dalton Trans.* **2003**, 3780.
- [18] S. Faulkner, B. P. Burton-Pye, *Chem. Commun.* **2005**, 259.
- [19] A. Congreve, D. Parker, E. Gianolio, M. Botta, *Dalton Trans.* **2004**, 1441.
- [20] C. Platas-Iglesias, D. M. Corsi, L. Vander Elst, R. N. Muller, D. Imbert, J.-C. Bünzli, É. Tóth, T. Maschmeyer, J. A. Peters, *Dalton Trans.* **2003**, 727.
- [21] S. Faulkner, personal communication.
- [22] L. Vander Elst, S. Laurent, R. N. Muller, *Invest. Radiol.* **1998**, *33*, 828.
- [23] a) G. Lipari, A. Szabo, *J. Am. Chem. Soc.* **1982**, *104*, 4546; b) G. Lipari, A. Szabo, *J. Am. Chem. Soc.* **1982**, *104*, 4559.
- [24] G. M. Nicolle, É. Tóth, K. P. Eisenwiener, H. R. Mäcke, A. E. Merbach, *J. Biol. Inorg. Chem.* **2002**, *7*, 757.
- [25] S. Torres, J. P. André, J. A. Martins, C. F. G. C. Geraldes, A. E. Merbach, É. Tóth, *Chem. Eur. J.* **2006**, *12*, 940.
- [26] É. Tóth, L. Helm, K. Kellar and A. E. Merbach, *Chem. Eur. J.* **1999**, *5*, 1202.
- [27] F. A. Dunand, É. Tóth, R. Hollister, A. E. Merbach, *J. Biol. Inorg. Chem.* **2001**, *6*, 247.
- [28] G. M. Nicolle, É. Tóth, H. Schmitt-Willich, B. Radüchel, A. E. Merbach, *Chem. Eur. J.* **2002**, *8*, 1040.
- [29] S. Laus, R. Ruloff, É. Tóth, A. E. Merbach, *Chem. Eur. J.* **2003**, *9*, 3555.
- [30] M.-R. Spirlet, J. Rebizant, J. F. Desreux, M.-F. Loncin, *Inorg. Chem.* **1984**, *23*, 359.
- [31] J. J. Stezowski, J. L. Hoard, *Isr. J. Chem.* **1984**, *24*, 323.
- [32] A. M. Raitsimring, A. V. Astashkin, D. Baute, D. Goldfarb, P. Caravan, *J. Phys. Chem. A* **2004**, *108*, 7318.
- [33] A. V. Astashkin, A. M. Raitsimring, P. Caravan, *J. Phys. Chem. A* **2004**, *108*, 1990.
- [34] L. Burai, É. Tóth, H. Bazin, M. Benmelouka, Z. Jászberényi, L. Helm, A. E. Merbach, *Dalton Trans.* **2006**, 629.
- [35] H. G. Hertz in *Water, a comprehensive treatise*, Vol. 77 (Ed.: F. Franks), Plenum, New York, **1973**, p. 685.
- [36] S. Laus, B. Sitharaman, É. Tóth, R. D. Bolskar, L. Helm, S. Asokan, M. S. Wong, L. J. Wilson, A. E. Merbach, *J. Am. Chem. Soc.* **2005**, *127*, 9368.
- [37] L. Burai, V. Hietapelto, R. Király, É. Tóth, E. Brücher, *Magn. Reson. Med.* **1997**, *38*, 146.
- [38] E. Brücher and A. D. Sherry, *Stability and Toxicity of Contrast Agents in The Chemistry of Contrast Agents in Medical Magnetic Resonance Imaging* (Eds.: É. Tóth, A. E. Merbach), Wiley, Chichester, **2001**, p. 243.
- [39] X. Zhang, C. A. Chang, H. G. Brittain, J. M. Garrison, J. Telser, M. F. Tweedle, *Inorg. Chem.* **1992**, *31*, 5597.
- [40] a) J. P. Collman, J. I. Brauman, J. P. Fitzgerald, P. D. Hampton, Y. Natura, J. W. Sparapany, J. A. Ibers, *J. Am. Chem. Soc.* **1988**, *110*, 3477; b) K. Kurz, M. W. Göbel, *Helv. Chim. Acta* **1996**, *79*, 1967.
- [41] G. Brunisholz, M. Randin, *Helv. Chim. Acta* **1959**, *42*, 1927.
- [42] C. Ammann, P. Meier, A. E. Merbach, *J. Magn. Reson.* **1982**, *46*, 319.
- [43] A. D. Hugi, L. Helm, A. E. Merbach, *Helv. Chim. Acta* **1985**, *68*, 508.
- [44] R. L. Vold, J. S. Waugh, M. P. Klein, D. E. Phelps, *J. Chem. Phys.* **1968**, *48*, 3831.
- [45] S. Meiboom, D. Gill, *Rev. Sci. Instrum.* **1958**, *29*, 688.
- [46] H. M. Irving, M. G. Miles, L. Pettit, *Anal. Chim. Acta* **1967**, *38*, 475.
- [47] L. Zékány, I. Nagypál in *Computation Methods for Determination of Formation Constants* (Ed: D. J. Leggett), Plenum, N.Y. (USA), **1985**, p. 291.
- [48] F. Yerly, *VISUALISEUR and OPTIMISEUR 2.3.4*, Université de Lausanne, Lausanne (Switzerland), **1999**.
- [49] K. Micskei, D. H. Powell, L. Helm, E. Brücher, A. E. Merbach, *Magn. Reson. Chem.* **1993**, *31*, 1011.
- [50] E. T. Clarke, A. E. Martell, *Inorg. Chim. Acta* **1991**, *190*, 37.
- [51] K. Kumar, C. A. Chang, M. F. Tweedle, *Inorg. Chem.* **1993**, *32*, 587.

Received: October 27, 2005

Revised: January 25, 2006

Published online: June 13, 2006